Purdue University
Purdue e-Pubs

CTRC Research Publications | Cooling Technologies Research Center

11-18-1998

Gas Dynamics and Electromagnetic Processes in High-Current Arc Plasmas - Part I: Model Formulation and Steady-State Solutions

Lei Z. Schlitz

S V. Garimella
Purdue Univ, sureshg@purdue.edu

S H. Chan

Follow this and additional works at: http://docs.lib.purdue.edu/coolingpubs

Schlitz, Lei Z.; Garimella , S V.; and Chan, S H., "Gas Dynamics and Electromagnetic Processes in High-Current Arc Plasmas - Part I: Model Formulation and Steady-State Solutions" (1998). *CTRC Research Publications.* Paper 84.
http://docs.lib.purdue.edu/coolingpubs/84

This document has been made available through Purdue e-Pubs, a service of the Purdue University Libraries. Please contact epubs@purdue.edu for additional information.

Gas dynamics and electromagnetic processes in high-current arc plasmas. Part I. Model formulation and steady-state solutions

Lei Z. Schlitz, Suresh V. Garimella,[a] and S. H. Chan
Department of Mechanical Engineering, University of Wisconsin–Milwaukee, P.O. Box 784, Milwaukee, Wisconsin 53201

(Received 19 August 1998; accepted for publication 18 November 1998)

A three-dimensional computational model has been developed to study the effects of self-induced and external magnetic fields, as well as gassing effects, on arcs involved in switching devices. A commercial computational fluid dynamics code has been adapted and modified to model the fully coupled plasma flow, heat transfer, and electromagnetic field. In this paper, a model is developed to analyze a steady-state, two-dimensional axisymmetric air arc column at low current levels under conditions in which the effects of the self-induced magnetic field are negligible. The model is then extended to analyze a three-dimensional arc column at high current levels with the inclusion of self-induced magnetic effects. The effects of cathode size, distance from the electrode, current level, self-induced magnetic field, and natural convection on the arc plasma are investigated. Predictions from these models compare favorably with published analytical and experimental results. The influence of external transverse magnetic fields, as well as the presence of gassing materials, on a three-dimensional arc column in both steady-state and transient situations will be discussed in L. Z. Schlitz *et al.* [J. Appl. Phys. **85**, 2547 (1999)]. © *1999 American Institute of Physics.* [S0021-8979(99)01805-8]

I. INTRODUCTION

Thermal plasmas have been the focus of a number of studies in the literature over the years. The generation of a thermal plasma and its stabilization are the major concerns in technological applications.[1] However, detailed numerical simulations of the complex plasma behavior have only recently become feasible with the availability of advanced computers.

The high-energy, high-intensity thermal plasma arc which develops between electrical contacts during circuit-interruption is a complicated phenomenon of great significance in the switching industry. The high-temperature and high-pressure arc dissipates the tremendous energy generated by fault current and hence, protects other parts of the circuit. At the same time, this energy has to be rapidly transferred away from the contacts in order to extinguish the arc and protect the neighboring components. In contrast to other applications involving thermal plasma technology, destabilization of the arc and arc motion are the essential areas of concentration in switching devices. Due to the highly transient nature of the arcs, as well as the complicated interactions between the arcs, the electrical field, and the contact materials, past investigations in the area have been largely limited to empirical observation.

Lowke and Ludwig[2] developed a simple model to simulate high-current arcs in a nozzle stabilized by forced convection. Simple, one-dimensional analytical expressions for arc motion were derived by Lowke[3,4] at both low and high currents using approximate properties of free-burning arc columns. A more sophisticated theoretical model of free-burning arcs was presented by Kovitya and Lowke[5] in which equations describing the conservation of mass, momentum, and energy were solved together with Ohm's law and Maxwell's equations for the magnetic field in a cylindrical coordinate system.

Since an arc is an electrically conducting medium, it will interact not only with its own self-induced magnetic field but also with externally applied magnetic fields. Magnetically deflected or stabilized arcs have attracted increasing attention and have been used extensively in the development of arc gas heaters for materials processing, in switchgear industries for the design of circuit breakers and contactors, and in arc furnaces.[1] Horinouchi *et al.*[6] presented a simple, practical method of simulating the behavior of arcs driven by magnetic forces for application in circuit breakers to study the arc-extinguishing capability of the interruption structure. However, plasma flow and heat transfer to and from the arc column were neglected. Speckhofer and Schmidt[7] developed a transient, three-dimensional simulation to study the influence of transverse magnetic fields on the arc column. Karetta and Lindmayer[8] developed a three-dimensional model of a switching arc in a low-voltage circuit breaker. A high-current arc column under atmospheric conditions between two parallel electrodes in a completely sealed arc chamber was modeled, in which the current density distribution at the electrodes was assumed to be a function of electrode temperature, and therefore, of time. Antisymmetry was assumed and only one electrode was modeled. With this model, arc motion under a transverse magnetic force, as well as the arc voltage, pressure, and temperature distribution inside the arc chamber, were predicted.

[a]Author to whom correspondence should be addressed: Cray-Research Associate Professor; electronic mail: sureshg@uwm.edu

 © 1999 American Institute of Physics

Downloaded 29 Aug 2001 to 128.46.190.93. Redistribution subject to AIP license or copyright, see http://ojps.aip.org/japo/japcr.jsp

In the present two-part paper, a model is developed which progressively evolves from a two-dimensional, axisymmetric, free-burning air arc plasma to a transient, three-dimensional arc under self-induced and external magnetic fields with cooling gases issuing from walls made of materials which sublimate at high temperatures. The model and code are validated through comparison with studies in the literature. Plasma temperature, arc voltage, current density, and pressure distribution are obtained for a variety of conditions.

Part I of this paper discusses the mathematical formulation of the model and the appropriate boundary conditions. A two-dimensional, axisymmetric, free burning air arc column at low current levels is first modeled without the inclusion of the self-induced magnetic field. A three-dimensional air arc column at high-current levels with the inclusion of the self-induced magnetic field is then simulated. The numerical predictions are compared to analytical and experimental results in the literature to establish confidence in the modeling approach.

Part II[9] of this paper describes the further development of the model to include external forces—external magnetic field and gassing materials—in a three-dimensional high-current air arc column. The simulation is time-dependent since the arcing behavior under these situations is highly transient and complex.

II. THE MATHEMATICAL MODEL

A macroscopic approach is used in this work to model the various plasma components. It is assumed that the plasma follows the conventional conservation equations for mass, momentum, and energy, which are described by the Navier–Stokes equations.[8,10] In addition, it is necessary for the simulation of the electric arc to include source terms in the momentum and energy equations which reflect the ohmic heating, radiative cooling, and the Lorentz force on the plasma due to self-induced and external magnetic fields. The electromagnetic processes are described by Maxwell's equations, which is another complex system of partial differential equations.[11] The following assumptions were made with respect to the thermal plasma column:[8]

(1) The plasma studied is assumed to be a thermal plasma which satisfies conditions for local thermodynamic equilibrium (LTE). Therefore, the plasma can be assumed to be optically thin.
(2) The plasma is considered to be a gas mixture with thermodynamic and transport properties obtained from the literature.[1,12] The physical properties (thermal conductivity, viscosity, density, specific heat, electrical conductivity, and effective volumetric emission coefficient) are functions of the plasma temperature and pressure.
(3) The plasma is assumed to be electrically neutral. Net charges are present in the vicinity of the cathode and the anode (which are responsible for the generation of electrons and ions). However, this so-called sheath region is ignored since the behavior of the plasma in the arc column is the focus of the present study, and its interaction with the surroundings is of primary importance in switching applications.
(4) It is assumed that the induced current is small compared to the injected current from the circuit; it is therefore neglected.
(5) The presence of ferromagnetic materials in the domain is disallowed, thus justifying the use of a constant permeability for the gaseous medium ($\mu_r = \mu_0$).

With these assumptions, Maxwell's equations may be simplified to consist of a current continuity equation describing the electrostatics, and a Biot–Savart equation to relate the electric and magnetic fields. It should be noted that the electromagnetic field and the fluid field are fully coupled. Therefore, the Navier–Stokes equations and Maxwell's equations have to be solved simultaneously.

When a plasma is under conditions of LTE, it can be assumed to be laminar and optically thin. Under such conditions, the appropriate governing equations are as follows, with ρ being density, μ dynamic viscosity, σ electron conductivity, ϕ electric potential, Φ viscous dissipation, h enthalpy, k thermal conductivity, q heat flux, S_R radiation source term, T temperature, t time, $\vec{g}$ gravitational acceleration, $\vec{V}$ velocity vector, p pressure, $\vec{J}$ electric current density, $\vec{B}$ magnetic flux density, and $\vec{E}$ electric field.

(1) Continuity:

$$\frac{\partial \rho}{\partial t} + \nabla \cdot (\rho \vec{V}) = 0 \tag{1}$$

(2) Momentum:

$$\frac{\partial \rho \vec{V}}{\partial t} + \nabla \cdot (\rho \vec{V} \vec{V}) = \vec{J} \times \vec{B} + \rho \cdot \vec{g} - \nabla p + \nabla \cdot \vec{\vec{\tau}}, \tag{2}$$

where, $\vec{\vec{\tau}}$ is the stress tensor:

$$\vec{\vec{\tau}} = \left[\mu \left(\frac{\partial V_i}{\partial x_j} + \frac{\partial V_j}{\partial x_i} \right) \hat{e}_i \hat{e}_j - \frac{2}{3} \vec{\vec{\delta}} \nabla \cdot \vec{V} \right]. \tag{3}$$

(3) Energy:

$$\frac{\partial \rho h}{\partial t} + \nabla \cdot (\rho \vec{V} h) = \nabla \cdot (k \nabla T) + \frac{\partial p}{\partial t} - S_R + \vec{J} \cdot \vec{E} + \Phi. \tag{4}$$

(4) Equation of State:

$$p = \rho R T. \tag{5}$$

(5) Current Continuity:

$$\nabla \cdot (\sigma \nabla \phi) = 0, \tag{6}$$

where ϕ may be expressed as

$$\vec{E} = -\nabla \phi, \tag{7}$$

$$\vec{J} = \sigma \cdot \vec{E} = -\sigma \cdot \nabla \phi. \tag{8}$$

(6) $\vec{B}$ is the magnetic flux density and can be calculated from the Biot–Savart equation:

Downloaded 29 Aug 2001 to 128.46.190.93. Redistribution subject to AIP license or copyright, see http://ojps.aip.org/japo/japcr.jsp

$$\vec{B}(\vec{r})=\vec{B}(\vec{r})_{\text{ext}}+\frac{\mu_0}{4\pi}\int\int\int_{V'}\vec{J}(\vec{r}')\times\frac{\vec{r}-\vec{r}'}{|\vec{r}-\vec{r}'|^3}dV'. \quad (9)$$

Equation (9) is used to calculate the magnetic flux density for a given current density distribution for each point $\vec{r}$ in the computational domain. The volume integral sums up the contribution of the current density $\vec{J}$ in any arbitrary volume dV' (at $\vec{r}'$) over the entire computational domain.

The source term in the momentum equation, $\vec{J}\times\vec{B}$, is the Lorentz force which represents the interaction between the electric current and the magnetic field. The magnetic field is a combination of self-induced and external components. The self-induced magnetic force is also called the ''pinch'' force and directs the plasma flow towards the arc center.

In an electrically conducting thermal plasma, an ohmic heating effect exists when there is electric current flowing through the plasma field.[1,13] The ohmic heating term $\vec{J}\cdot\vec{E}$ in Eq. (4) is a major factor in causing the high temperatures found in electric arcs. The greater the current density, the larger is the heat generation due to ohmic heating; so also, the more electrically resistive the plasma, the larger is the heat generation.

Thermal radiation plays a significant role in switching arcs due to the high operating temperatures (>5000 K). The formulation of energy transport by thermal radiation is very complicated. The spectrum is composed of both continuous and line spectra, where the lines are determined by the energy levels of the atoms and molecules in the plasma. Furthermore, the dependence of radiative properties on temperature and pressure must also be considered.[14] In this study, since the thermal plasma satisfies LTE and is thus optically thin, it is possible to use a source term (S_R) in the energy Eq. (4) to represent the radiation effects. This term S_R represents the total volumetric emission coefficient. The estimates of Johnston *et al.*[12] for the total emission coefficient as functions of temperature and pressure are used here.

A. Numerical analysis

In order to solve the system of differential equations with complex temperature- and pressure-dependent properties, the computational fluid dynamics (CFD) code FLUENT[15] has been adapted and used. FLUENT is a finite-volume based computer program that models fluid flow, heat transfer, and chemical reaction. The program uses a general curvilinear grid to divide the computational domain into discrete control volumes and integrate the governing equations on the individual control volumes to construct algebraic equations for the discrete unknowns. The SIMPLEC algorithm[16] is used to relate the pressure and velocity fields. A multigrid scheme is utilized to accelerate the line-by-line iterative solver.

User-defined subroutines are added to the program to implement the extra transport Eq. (6) and the source terms in Eqs. (7) to (9). Subroutines are also implemented to allow thermodynamic and transport properties to be functions of temperature and pressure. User-defined variables, such as $\vec{J}$ and $\vec{B}$ are also calculated in the subroutines. The partial differential equations are solved together to obtain the plasma pressure, velocity field, temperature, and electrical properties. The calculation depends only on the electrode shape, the distance between electrodes, the input current, current density, the external magnetic field, and the material properties of the plasma as functions of temperature and pressure. Under-relaxation factors are used for all dependent variables and physical properties to ensure fast solution convergence.

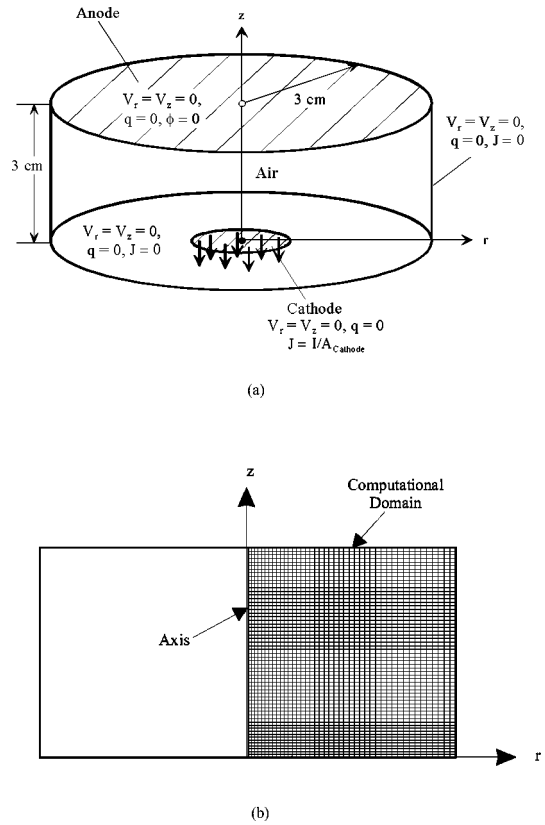

FIG. 1. (a) Schematic diagram of a low-current free burning arc in a two-dimensional axisymmetric configuration showing coordinate system and boundary conditions; and (b) computational grid used in the simulation.

The plasma flow, heat transfer, and electromagnetic fields are fully coupled. The development of the model and validation of the software is organized into two stages as described below: a two-dimensional, axisymmetric arc, and a three-dimensional arc column. Additional details are available in Schlitz.[17]

1. Two-dimensional arc column (no magnetic field)

The first simulation was for a two-dimensional arc column including the effect of only the electric field on the plasma (ohmic heating). The magnetic field is excluded from this model, with the effect of the Lorentz force on the plasma flow [source term in Eq. (2)] assumed to be negligible. This assumption is reasonable at low current levels (<100 A) in air, when any influence of the self-induced magnetic field is small[3] compared to other effects, such as air flow due to natural convection. In fact, for low-current arcs, the controlling physical process is natural convection. With this assumption, a two-dimensional axisymmetric problem was set up as shown in Fig. 1.

The anode is the upper plate in Fig. 1(a) with a radius of 30 mm, while the cathode (R_{cath}) is 30 mm below the anode

Downloaded 29 Aug 2001 to 128.46.190.93. Redistribution subject to AIP license or copyright, see http://ojps.aip.org/japo/japcr.jsp

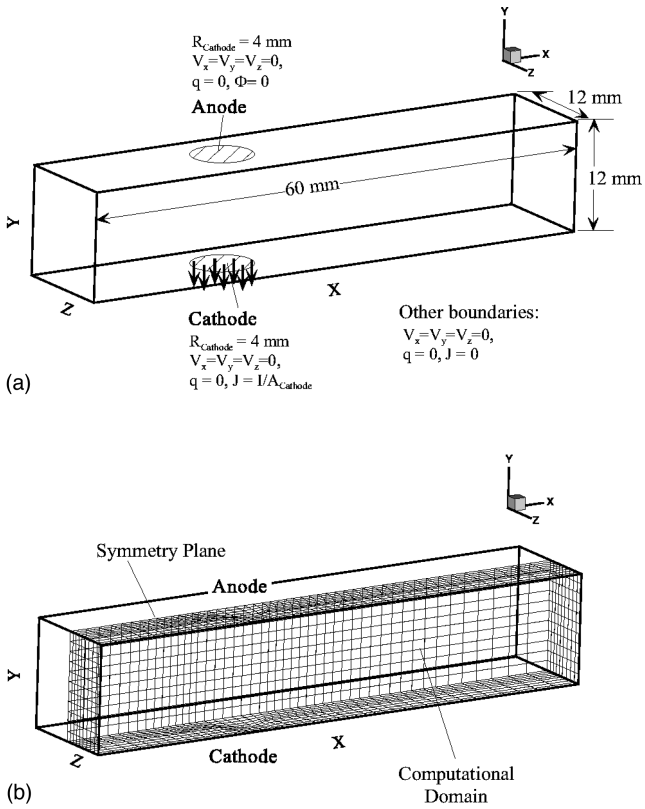

FIG. 2. (a) Schematic diagram of a high-current free burning arc in a three-dimensional configuration showing coordinate system and boundary conditions; and (b) computational grid used in the simulation.

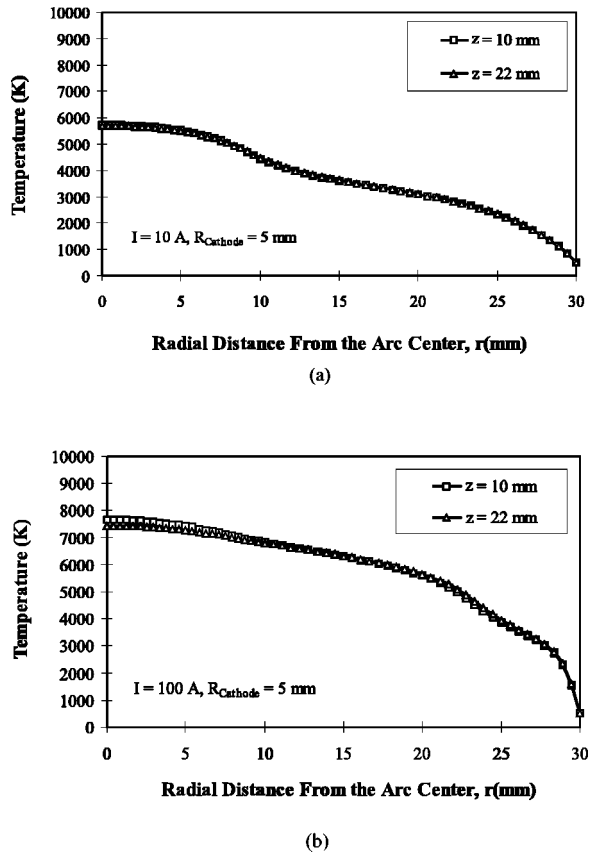

FIG. 3. Effect of the distance from the cathode on the radial temperature distribution of the two-dimensional axisymmetric free burning arc in air without a magnetic force for $R_{cath}=5$ mm, and (a) $I=10$ A, and (b) $I=100$ A.

and has one of two values for radius: 5 or 10 mm. The cathode has a uniformly distributed current flow, while the anode is a collector for negative particles (electrons and negative ions) and has a uniform electrical potential on the surface (and not uniform current density). Since the electrodes themselves are not modeled in the analysis, the behavior of the arc near the surface does not necessarily correspond to reality. Away from the electrodes, however, inside the arc column, conclusions drawn from the model are valid. The computational domain is enclosed and allows no mass transfer with the exterior. The boundary conditions used in this model are also shown in Fig. 1(a). Natural-convection effects are included in all the simulations, i.e., the gravitational force is in the $-x$ direction. Four cases are considered with current levels of 10 and 100 A for each of the two cathode radii (5 and 10 mm).

The computational mesh used in the simulations is shown in Fig. 1(b), with the z-axis being the axis of symmetry. The cathode and anode are located on the lower and upper boundaries, respectively. The mesh size $(r\times z)$ is 44×61. The computations were performed on a SGI IndigoII R10 000 workstation. For the two-dimensional axisymmetric computations without inclusion of the self-induced magnetic field, the average CPU consumption was 3 mins.

2. Three-dimensional arc column with and without a magnetic field

At high current levels (>100 A), the self-induced magnetic field cannot be neglected.[3] In this model, both the cathode and anode are 8 mm in diameter, and the physical domain is $60\times12\times12$ mm as shown in Fig. 2(a); a grid size of $49\times13\times11$ is used as illustrated in Fig. 2(b). The arc chamber is enclosed and no mass transfer is permitted with the outside. Taking advantage of symmetry, only half the domain is modeled computationally. The specific geometry was chosen to match that of experimental results in the literature so as to facilitate comparisons. In order to demonstrate the

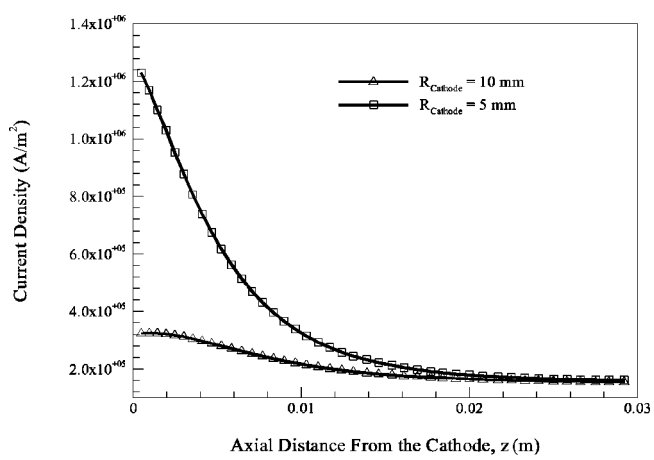

FIG. 4. Effect of the cathode diameter on the arc centerline current density for the two-dimensional axisymmetric free burning arc in air without a magnetic force for $I=10$ A.

Downloaded 29 Aug 2001 to 128.46.190.93. Redistribution subject to AIP license or copyright, see http://ojps.aip.org/japo/japcr.jsp

TABLE I. Arc temperature, arc radius, field strength, and plasma velocity 10 mm from the cathode at the arc centerline for the two-dimensional axisymmetric air plasma arc with natural convection.

Current I (A)	R_{cath} (mm)	Arc temperature (K)	Arc radius (nm) 95% current	Arc radius (nm) 90% current	Field (V/cm)	Plasma velocity (mm/s)
100	10	7200	21.1	19.4	9.3	20.1
100	5	7270	21.1	19.5	9.3	20.4
10	10	5630	13.3	11.7	17	53.5
10	5	5680	11.4	9.9	17	54

importance of the self-induced magnetic field, cases with and without the inclusion of this field are modeled for each of three current levels studied: 700, 1000, and 1800 A. For high-current levels, it was found that the magnetic force has to be included in the calculations via the source term for the Lorentz force in Eq. (2). The magnetic field is calculated once the electric field and current density are known from the Biot–Savart equation.

The computations for the three-dimensional cases were performed on the 4-processor SGI Power Challenge R10 000 server. The CPU time for a typical run was 60 min.

III. RESULTS AND DISCUSSION

Results from the two- and three-dimensional computational models are presented in this section to illustrate the effects of cathode size, distance from the electrode, current level, self-induced magnetic field, and natural convection on the arc plasma. The predicted results are compared to analytical and experimental results from the literature.

A. Two-dimensional arc column (no magnetic field)

In order to characterize low-current arcs, the influence of axial distance from the electrode and of cathode size are illustrated. Figures 3(a) and 3(b) show the radial distribution of plasma temperature at different axial distances from the cathode surface (10 and 22 mm) for a cathode diameter of 5 mm, at two different current levels of 10 and 100 A, respectively. The temperature at the center of the arc reaches 5680 and 7270 K for the two current levels, dropping gradually with distance away from the axis to less than 1000 K at the boundary. The temperatures at different axial distances from the cathode almost coincide with each other for a given current level, showing that the arc is not affected by the electrode at distances farther than 10 mm from the cathode; under these conditions, the arc may be classified as an ''arc column.'' (It is to be noted that since the anode serves only as an electron-receiving plate with constant electric potential, distance from the anode would not be a parameter of significance.) The absence of electrode effects on the arc behavior some distance from the electrodes has been recognized in the literature;[3] it has been shown that an axisymmetric arc column may be simulated using a one-dimensional model which excludes the electrodes.

The effect of electrode size on the arc may be demonstrated by examining the centerline (r = 0) current density for different arc root diameters. Figure 4 shows current density along the arc centerline for $R_{cath}=5$ and 10 mm at $I=100$ A. The cathode and anode are at the left and right extremes of this graph respectively ($z=0$ and 0.03 m). The current density is greatest at the cathode, dropping off to a near-constant level ($\approx 1.9\times 10^5$ A/m^2) beyond a distance of 13 mm from the cathode for both arc root diameters. However, the magnitude of current density at the cathode for the smaller cathode is over 1.2×10^6 A/m^2, a value over three times higher than that for the larger cathode (3.2×10^5 A/m^2). This figure also demonstrates that arc-column behavior is reached at axial distances from the cathode beyond 10 to 13 mm.

A summary of the results from these calculations is presented in Table I. The arc (centerline) temperature, arc radius, field strength (voltage drop between the electrodes), and plasma velocity due to natural convection are shown in the table. It should be noted that the arc is defined as the region where there is current flow. In the case of a two-dimensional axisymmetric domain, the radius of the region that surrounds 90% of the total current is considered to be the arc radius. Also, since the analysis is to be compared to other analytical and experimental results which do not necessarily have the same geometry of electrodes as in the current study, the present results are considered in a region far enough ($\geqslant$10 mm) from the cathode to have a negligible influence from the electrodes.

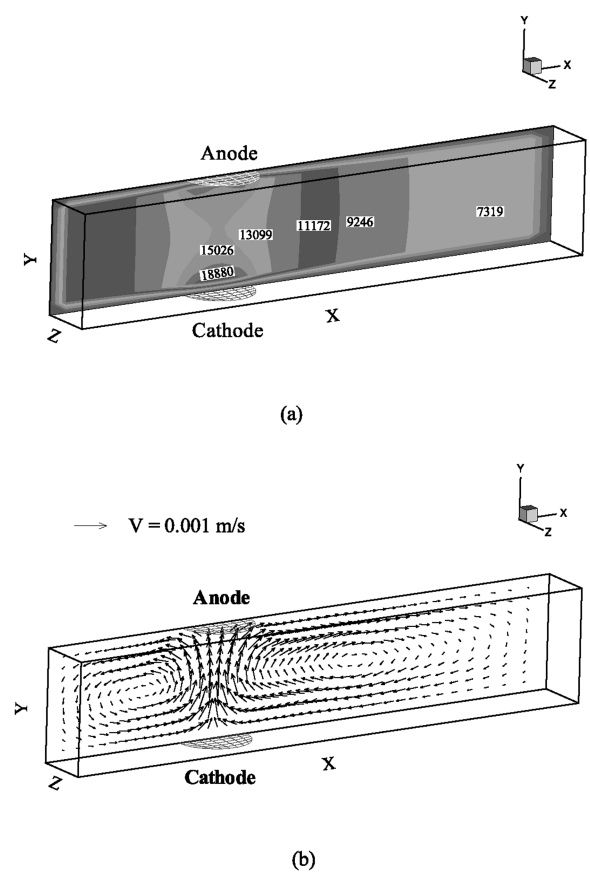

FIG. 5. (a) Temperature contours and (b) plasma velocity vectors in a three-dimensional air arc column at the symmetry plane ($z=0$), without the inclusion of the self-induced magnetic field for a current level of 1000 A.

Downloaded 29 Aug 2001 to 128.46.190.93. Redistribution subject to AIP license or copyright, see http://ojps.aip.org/japo/japcr.jsp

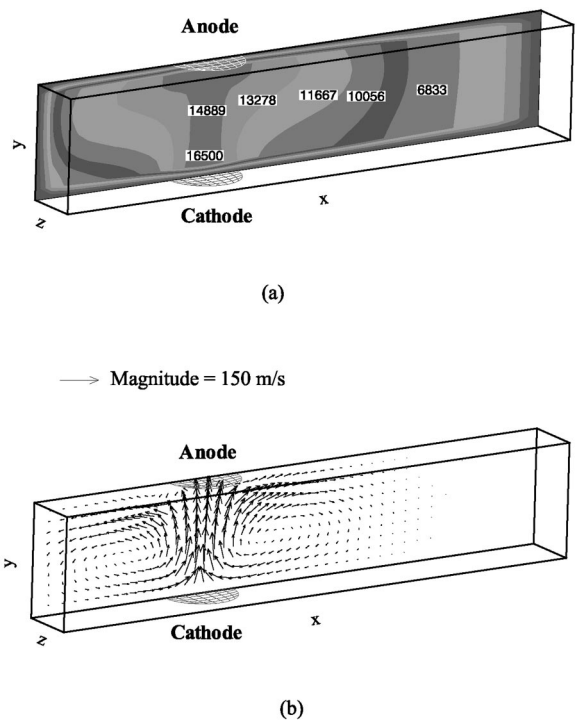

FIG. 6. (a) Temperature contours and (b) plasma velocity vectors in a three-dimensional air arc column at the symmetry plane ($z=0$), with the inclusion of the self-induced magnetic field for a current level of 1000 A.

B. Three-dimensional arc column with and without a magnetic field

The three-dimensional arc column was investigated as discussed earlier (Fig. 2) for three different current levels, $I=700$, 1000, and 1800 A. At high current levels (>100 A), the self-induced magnetic field created by the electrically conducting arc may no longer be neglected. This is demonstrated by a comparison of Figs. 5 and 6, showing results obtained without and with the inclusion of this magnetic field, respectively. With the magnetic force excluded (Fig. 5), the plasma temperature and flow fields are dominated by natural convection, with the high-temperature region being symmetric about the midplane between the two electrodes and bearing the shape of an hourglass. The maximum gas velocity due to natural convection in this case is of the order of 0.001 m/s. When the self-induced magnetic field is included in the calculations (Fig. 6), the large pinch force causes the electrodes to serve as gas pumps and induces plasma jets from both electrodes towards the middle (the anode jet is not distinctly seen in the figure since it is overwhelmed by the much larger cathode-jet induced flow). The two electrode jets collide and flow outward, away from the arc centerline. The maximum velocity in the plasma field is 152 m/s. This is several orders of magnitude higher than that from pure natural convection, which clearly indicates a magnetic-force-dominated situation. The vigorous plasma flow [Fig. 6(b)] causes the high-temperature region ($>10\,000$ K) to reflect the shape of the gas jets issuing outward in the vicinity of the anode. The outward-flow plasma jets are not located exactly midway between the electrodes due to the different electrical boundary conditions at the electrodes (the cathode has uniform J, while the anode has $\phi=0$). Simulations performed at current levels of $I=700$ and 1800 A with and without inclusion of the self-induced magnetic field yield similar conclusions.

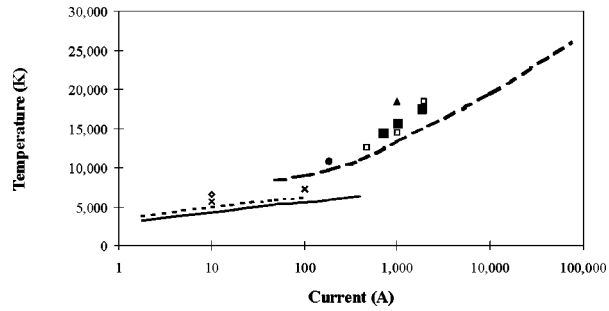

FIG. 7. Comparison of the predicted (■×) arc centerline temperatures 10 mm from the cathode as a function of current for air at 1 atm with those from Lowke (see Ref. 3) (solid and dotted lines for low current with natural convection using different temperature profiles, and dashed line for high current with self-induced magnetic field); Sperling (see Ref. 18) (◇); Maecker (see Ref. 19) (●); Slade and Schulz-Gulde (see Ref. 20) (△); and Bowman (see Ref. 21) (□).

In order to validate the computations, results from the present study are compared with analytical and experimental studies in the literature, in terms of arc temperature, diameter and field strength at different current levels; comparisons are made for all quantities at a distance of 10 mm from the cathode surface. Figure 7 shows these comparisons for arc temperature as a function of current. The theoretical predictions from the literature[3] shown in the comparisons considered low-current (<30 A) arcs, in which the controlling physical process was assumed to be natural convection. The arc was vertical and the input electrical energy produced an arc plasma which was carried upward by natural convection. The solid and dotted lines show these results with the inclusion of natural convection using a channel and a parabolic model respectively for the temperature profile. Lowke[3] also modeled high-current (>100 A) arcs; these results are shown in Fig. 7 as a dashed line. Also shown in the figure are experimental results collected by Lowke[3] from various studies (as identified in the figure caption). Reasonable agreement is seen in Fig. 7 between results from the present study and those in the literature.

Comparisons for the arc diameter are shown in Fig. 8.

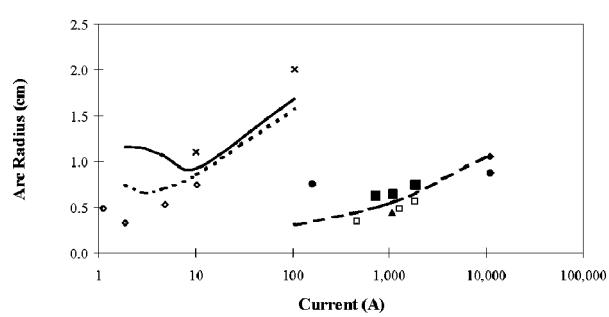

FIG. 8. Comparison of the predicted (■×) arc radius 10 mm from the cathode as a function of current for air at 1 atm with results from Lowke (see Ref. 3); lines and symbols are as used in Fig. 7, along with Suits (see Ref. 22) (◇) and Ramakrishnan and Stokes (see Ref. 23) (♦).

Downloaded 29 Aug 2001 to 128.46.190.93. Redistribution subject to AIP license or copyright, see http://ojps.aip.org/japo/japcr.jsp

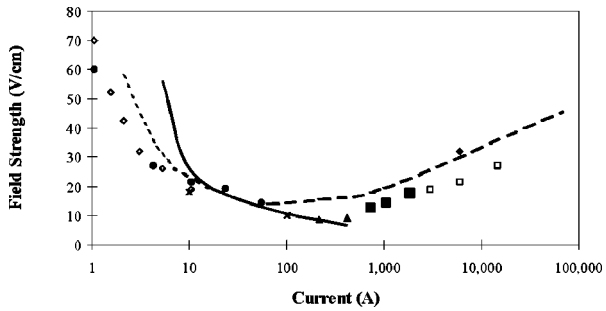

FIG. 9. Comparison of the predicted (■×) field strength 10 mm from the cathode as a function of current for air at 1 atm with results from Lowke (see Ref. 3); lines and symbols are as used in Fig. 7, along with Rieder (see Ref. 24) (●), Nicolai (see Ref. 25) (△), and Strachan (see Ref. 26) (□).

The discontinuity in arc diameter at 100 A in the analytical results in the figure is brought about by two different models (low-current and high-current) being used in calculating arc diameter. In reality, the arc diameter would fall between the predictions from the two models.

The predicted field strengths are compared with results from the literature in Fig. 9, in which field strength is defined as the voltage drop along the arc centerline per unit length. This definition excludes the effect of the voltage drop in the sheath regions, and therefore, is a good measure of the arc strength in an arc column where electrode and axial effects are not considered. Again, the agreement of the predicted results with the literature is satisfactory.

IV. SUMMARY

A numerical model has been formulated to simulate two- and three-dimensional air arc columns with and without the inclusion of the self-induced magnetic field. The arc temperature is largely independent of distance from the cathode in the so-called arc column region at distances of greater than 10 mm from the cathode. The current density is highest at the cathode and drops off with distance from the cathode. The current density adjacent to the cathode is significantly higher for a smaller cathode radius; however, current densities for both small and large cathodes drop to comparable values when arc column behavior is reached. The results from this study show that when the current levels are low, the contribution of the self-induced magnetic field is negligible, while at high current levels (>100 A), the pinch effect produced by this field can no longer be neglected. The strong interactions between the plasma flow field and the electromagnetic field are well resolved by the model, as is the behavior of the arc in the presence of a magnetic force under high-current situations. The predictions from the present study compare favorably with analytical and experimental results in the literature. This validated model is used in Part II (Ref. 9) of this work to study the influence on arc motion of external magnetic fields and gassing materials.

[1] M. I. Boulos, P. Fauchais, and E. Pfender, *Thermal Plasmas—Fundamentals and Applications* (Plenum, New York, 1994), Vol. 1.
[2] J. J. Lowke and H. C. Ludwig, J. Appl. Phys. **46**, 3352 (1975).
[3] J. J. Lowke, J. Phys. D: Appl. Phys. **12**, 1873 (1979).
[4] J. J. Lowke, J. Appl. Phys. **50**, 147 (1979).
[5] P. Kovitya and J. J. Lowke, J. Phys. D: Appl. Phys. **18**, 53 (1985).
[6] K. Horinouchi, Y. Nakayama, M. Hidake, T. Yonezawa, and H. Sasao, *IEEE/PES Summer Meeting*, Denver, CO, 26 July–1 August, 1996.
[7] G. Speckhofer and H. P. Schmidt, IEEE Trans. Plasma Sci. **24**, 1239 (1996).
[8] F. Karetta and M. Lindmayer, *42nd IEEE-Holm Conference on Electrical Contacts*, Chicago, IL, September 16–20, 1996.
[9] L. Z. Schlitz, S. V. Garimella, and S. H. Chan, J. Appl. Phys. **85**, 2547 (1999).
[10] J. J. Lowke, P. Kovitya, and H. P. Schmidt, J. Phys. D: Appl. Phys. **25**, 1600 (1992).
[11] W. H. Hayt, Jr., *Engineering Electromagnetics* (McGraw-Hill, New York, 1989).
[12] R. R. Johnston, O. R. Platas, and L. M. Tannenwald, *LMSC Technical Report No. N-3L-70-1* (1970).
[13] M. N. Hirsh and H. J. Oskam, *Gaseous Electronics, Electrical Discharges* (Academic, New York, 1978), pp. 290–398, Vol. 1.
[14] M. F. Modest, *Radiative Heat Transfer* (McGraw-Hill, New York, 1994).
[15] Fluent Inc., FLUENT User's Manual (Lebanon, New Hampshire, 1996).
[16] S. V. Patankar, *Numerical Heat Transfer and Fluid Flow* (McGraw-Hill, New York, 1980).
[17] L. Z. Schlitz, Ph.D. thesis, University of Wisconsin-Milwaukee, 1998.
[18] J. Sperling, Z. Phys. **128**, 269 (1950).
[19] H. Maecker, Z. Phys. **136**, 119 (1953).
[20] P. G. Slade and E. Schulz-Gulde, J. Appl. Phys. **44**, 157 (1973).
[21] B. Bowman, J. Phys. D: Appl. Phys. **5**, 1422 (1972).
[22] C. G. Suits, J. Appl. Phys. **10**, 730 (1939).
[23] S. Ramakrishnan and A. D. Stokes, J. Appl. Phys. **45**, 5480 (1974).
[24] W. Rieder, Z. Phys. **146**, 629 (1956).
[25] L. Nicolai, Phys. Fluids **13**, 2983 (1970).
[26] D. C. Strachan, *Proceedings of the 12th International Conference Phenomena in Ionized Gases*, Eindhoven 150 (North-Holland, Amsterdam, 1975).

Downloaded 29 Aug 2001 to 128.46.190.93. Redistribution subject to AIP license or copyright, see http://ojps.aip.org/japo/japcr.jsp